

## Article

# Ce and Y Co-Doping Effects for $(\text{Ba}_{0.85}\text{Ca}_{0.15})(\text{Zr}_{0.1}\text{Ti}_{0.9})\text{O}_3$ Lead-Free Ceramics

Chao Li <sup>1</sup>, Jin-Su Baek <sup>2</sup> and Jung-Hyuk Koh <sup>1,2,\*</sup>

<sup>1</sup> Department of Intelligent Energy and Industry, Chung-Ang University, Seoul 06974, Korea; a5995661@naver.com

<sup>2</sup> School of Electrical and Electronics Engineering, Chung-Ang University, Seoul 06974, Korea; choith70@naver.com

\* Correspondence: jhkoh@cau.ac.kr; Tel./Fax: +82-2-820-5311

**Abstract:**  $\text{CeO}_2$  and  $\text{Y}_2\text{O}_3$  were co-doped to  $(\text{Ba}_{0.85}\text{Ca}_{0.15})(\text{Zr}_{0.1}\text{Ti}_{0.9})\text{O}_3$  ceramics and sintered by conventional solid-state reaction process to form x wt.%  $\text{CeO}_2$ -y wt.%  $\text{Y}_2\text{O}_3$  doped  $(\text{Ba}_{0.85}\text{Ca}_{0.15})(\text{Zr}_{0.1}\text{Ti}_{0.9})\text{O}_3$  ( $\text{Ce}_x\text{Y}_y\text{-BCZT}$ ) ceramics. The effects of different contents of  $\text{CeO}_2$ - $\text{Y}_2\text{O}_3$  dopants to the  $(\text{Ba}_{0.85}\text{Ca}_{0.15})(\text{Zr}_{0.1}\text{Ti}_{0.9})\text{O}_3$  composition were analyzed by studying the phase, surface microstructure, piezoelectric and ferroelectric properties of BCZT ceramics. In this study, we have shown that co-doping a small amount of  $\text{CeO}_2$  and  $\text{Y}_2\text{O}_3$  will not change the phase structure of  $(\text{Ba}_{0.85}\text{Ca}_{0.15})(\text{Zr}_{0.1}\text{Ti}_{0.9})\text{O}_3$  ceramics. However, the proper introduction of  $\text{CeO}_2$  and  $\text{Y}_2\text{O}_3$  can improve the piezoelectric constant and electromechanical coupling coefficient of BCZT ceramic samples. Moreover, these dopants can promote the grain growth process in  $(\text{Ba}_{0.85}\text{Ca}_{0.15})(\text{Zr}_{0.1}\text{Ti}_{0.9})\text{O}_3$  ceramics.  $\text{Ce}_{0.04}\text{Y}_{0.02}$  doped  $(\text{Ba}_{0.85}\text{Ca}_{0.15})(\text{Zr}_{0.1}\text{Ti}_{0.9})\text{O}_3$  ceramic has the best piezoelectric properties compared with other composition, the results are as follows: Relative density = 96.9%,  $K_p = 0.583$ , and  $d_{33} = 678$  pC/N,  $V = 8.9$  V. It means that this  $\text{Ce}_{0.04}\text{Y}_{0.02}$  doped  $(\text{Ba}_{0.85}\text{Ca}_{0.15})(\text{Zr}_{0.1}\text{Ti}_{0.9})\text{O}_3$  ceramic is a desired material in the application of lead-free ceramics.



**Citation:** Li, C.; Baek, J.-S.; Koh, J.-H. Ce and Y Co-Doping Effects for  $(\text{Ba}_{0.85}\text{Ca}_{0.15})(\text{Zr}_{0.1}\text{Ti}_{0.9})\text{O}_3$  Lead-Free Ceramics. *Coatings* **2021**, *11*, 1248. <https://doi.org/10.3390/coatings11101248>

Academic Editor: Roman A. Surmenev

Received: 7 September 2021  
Accepted: 9 October 2021  
Published: 14 October 2021

**Publisher's Note:** MDPI stays neutral with regard to jurisdictional claims in published maps and institutional affiliations.



**Copyright:** © 2021 by the authors. Licensee MDPI, Basel, Switzerland. This article is an open access article distributed under the terms and conditions of the Creative Commons Attribution (CC BY) license (<https://creativecommons.org/licenses/by/4.0/>).

**Keywords:** lead-free ceramics; co-doped; piezoelectric

## 1. Introduction

In the past few decades, lead zirconate titanate (PZT) ceramics have been widely employed in piezoelectric device applications due to their high piezoelectric charge coefficient ( $d_{33} = 220\text{--}590$  pC/N), electromechanical coupling coefficient ( $k_p = 0.5\text{--}0.7$ ), and high Curie temperature ( $T_c = 550$  °C). However, these attractive PZT ceramics have some kinds of drawbacks in volatile and toxic properties [1,2]. During the sintering process, it will volatilize quickly if the temperature exceeds 880 °C, which creates defects in the structure. Therefore, electrical properties can be degenerated due to stoichiometric imbalance. In addition, to overcome toxic and related environmental problems, many attempts have been made. Among these attempts, research on lead-free materials has been increased. In order to achieve the goal of eco-friendly and sustainable development for piezoelectric materials, the new development of lead-free ceramics and PVDF piezoelectric film with excellent performance is essential for human beings [3–8]. PVDF piezoelectric film also has high chemical stability, soft texture, and lightweight merits [9].

As lead-free piezoelectric ceramics,  $(\text{Ba}_{0.85}\text{Ca}_{0.15})(\text{Zr}_{0.1}\text{Ti}_{0.9})\text{O}_3$  (hereafter BCZT) ceramics have strong merits in the piezoelectric device applications due to their high piezoelectric charge coefficient of 600 pC/N and electro-mechanical coupling coefficient of 0.5 [10,11]. One of the family materials of  $\text{BaTiO}_3$  piezoelectric ceramics, BCZT ceramics, have substituted components of Ca and Zr for A and B site of the perovskite structure. Due to the substituted materials of Ca and Zr in the perovskite structure, partial strains were developed in the lattice parameters of substituted BCZT ceramics. Due to this controlled strain in the perovskite structure, piezoelectric properties can be increased. Since there are

no volatile elements in the BCZT composition, BCZT can well maintain the pre-designed stoichiometric composition even after a high sintering temperature process. Especially, BCZT has an environmentally friendly composition and has a large relative dielectric constant, high residual polarization strength, low dielectric loss, and piezoelectric performance comparable to PZT-based ceramics. Therefore, it is one of the most promising lead-free piezoelectric ceramic systems to replace lead-containing materials [12–14]. The core performance of piezoelectric ceramics is the piezoelectric charge coefficient and electromechanical coupling coefficient. Having excellent piezoelectric charge coefficient and electromechanical coupling coefficient can make piezoelectric materials for good energy harvesting devices with high performance. Researchers have made many efforts to improve the piezoelectric properties of BCZT ceramics. For example, Wang et al. studied the effects of various rare earth elements on the piezoelectric properties of BCZT ceramics, and the increased piezoelectric properties ranged from 475 to 521 pC/N [15]. Generally, to maintain electrical neutrality, donor doping will form a certain amount of cation vacancies in the BCZT lattice. These cation vacancies will promote the movement of the electric domain wall during the polarization process. Thus, that the number of domains oriented along the direction of the electric field increases, thereby increasing Piezoelectric properties of piezoelectric ceramics, electromechanical coupling coefficient. Therefore, the purpose of this research is to co-doped two kinds of donor doping elements to obtain BCZT ceramics with dual donor doping effects and high-voltage electrical coefficients.

## 2. Materials and Methods

BaCO<sub>3</sub> (purity 99%, High Purity Chemicals KOJUNDO CHEMICAL LABORATORY Co., Ltd., Chiyoda, Sakado, Japan), CaCO<sub>3</sub> (purity 99.0%, Sigma-Aldrich Co., Ltd., St. Louis, MO, USA), TiO<sub>2</sub> (purity 99.9%), ZrO<sub>2</sub> (purity 99.0%), CeO<sub>2</sub>, Y<sub>2</sub>O<sub>3</sub> are raw materials, and x wt.% CeO<sub>2</sub> y wt.% Y<sub>2</sub>O<sub>3</sub>—(Ba<sub>0.85</sub>Ca<sub>0.15</sub>) (Ti<sub>0.9</sub>Zr<sub>0.1</sub>) O<sub>3</sub>—(Ce<sub>x</sub>Y<sub>y</sub>-BCZT) ceramic powder is prepared by a conventional solid-state reaction method. These starting powders were weighed according to the stoichiometric ratio and then ball milled with ethanol and zirconia balls for 24 h. After drying for 12 h at 120 °C, the mixture was calcined at 1300 °C for 2 h. Subsequently, these powders were mixed with polyvinyl alcohol (PVA) as a binder and pressed into a (12 mm × 1.2 mm). The thick films were prepared by the milling process. The thickness of thick films was measured and controlled by the vernier calipers. After the PVA was burned, it was sintered at a temperature of 1450 to 1550 °C for 4 h. To characterize its dielectric and piezoelectric properties, the sample was screen printed with silver paste on the top and bottom and cured at 700 °C for 10 min. Polarize these samples in silicone oil at 30 °C and 30–40 kV/cm for 20 min. X-ray diffraction (XRD, D8-Advance/Bruker-AXS, Karlsruhe, Germany) was used to study and analyze the crystal structure. The piezoelectric constant  $d_{33}$  was determined by the Berlin court type quasi-static meter. The cross-section of the sample was etched at a temperature 150 °C lower than the sintering temperature of the sample for 60 min. Observe the microstructure of the sample by scanning electron microscope (FE-SEM, SIGMA 300, Carl Zeiss, Jena, Germany). When observing the microstructure of the sample in the FE-SEM system, the operating conditions were as follows, magnification: 1000 or 5000 times, working distance: 6.8 mm, acceleration voltage: 5.00 KV, image resolution pixel: 1024 × 768 pixels. Through measurement and calculation, the volume density and relative density were obtained.

## 3. Result and Discussion

In order to study the influence of different sintering temperatures on Ce<sub>0.04</sub>Y<sub>0.02</sub>-BCZT ceramics, XRD measurements were performed at the sintering temperature between 1450 and 1550 °C.

Figure 1 shows the sintering temperature dependent X-ray diffraction patterns of Ce<sub>0.04</sub>Y<sub>0.02</sub>-BCZT ceramics. It was observed that the peaks position of Ce<sub>0.04</sub>Y<sub>0.02</sub>-BCZT ceramics have perovskite structure without any pyrochlore phase. This indicates that co-dopants of Ce and Y diffuse into the BCZT ceramic lattice without destroying the

original crystal structure and forming a solid solution [16]. As shown in Figure 1, the reflection of (211) peaks moved to the lower angle as the sintering temperature increased. This means that unit cell volume was increased as the sintering temperature increased. However, the sintering temperature rises from 1500 to 1550 °C, reflection of (211) peaks almost no movement. This shows that, compared to other sintering temperatures, 1500 °C was the most helpful for ion substitution and solid solution formation, thus it reached the maximum at 1500 °C.

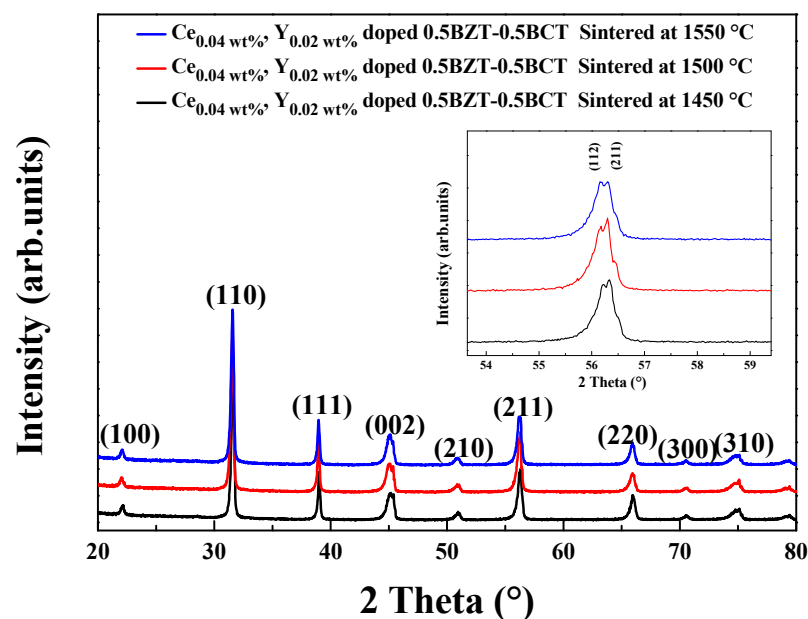


**Figure 1.** Sintering temperature-dependent X-ray diffraction patterns of  $\text{Ba}_{0.85}\text{Ca}_{0.15}(\text{Zr}_{0.1}\text{Ti}_{0.9})\text{O}_3\text{-Ce}_{0.04}\text{Y}_{0.02}$  ceramics. The insert is a peak shift of (211) for different sintering temperatures from 1450 to 1550 °C.

Figure 2 shows the sintering temperature-dependent piezoelectric charge coefficient of  $d_{33}$  and electromechanical coupling coefficient of  $k_p$  for  $\text{Ce}_{0.04}\text{Y}_{0.02}\text{-BCZT}$  ceramics. The sintering temperature-dependent properties of  $d_{33}$  and  $K_p$  showed similar behavior to each other. First, as the sintering temperature increased, the  $d_{33}$  and  $k_p$  of  $\text{Ce}_{0.04}\text{Y}_{0.02}\text{-BCZT}$  ceramics increased from 620 pC/N and 0.535 to 678 pC/N and 0.583 at 1450 °C and 1500 °C, respectively. Then, when the temperature reached 1550 °C, the piezoelectric performance and electromechanical coupling coefficient of  $\text{Ce}_{0.04}\text{Y}_{0.02}\text{-BCZT}$  ceramics began to decrease. This sintering temperature-dependent behavior of  $d_{33}$  and  $k_p$  can be explained by the principle of ceramic sintering. The main purpose of the sintering process was to promote the full growth of ceramic grains [17]. During the sintering process, grain size became larger with reducing the porosity. However, when the sintering temperature reached 1550 °C, over sintering process began to start. Many grains grow abnormally without stoichiometric composition due to the excessively high sintering temperature. Therefore, grain distribution became irregular, resulting in many defects and reduced density. Therefore, the piezoelectric properties and electromechanical coupling coefficient of ceramics deteriorate when the sintering temperature was 1550 °C. Based on Figure 2, it seems that the best piezoelectric properties of  $\text{Ce}_{0.04}\text{Y}_{0.02}\text{-BCZT}$  ceramics were when the sintering temperature was around 1500 °C. Therefore, based on this result, co-doping effects of Ce and Y to BCZT were analyzed at the sintering temperature near 1500 °C.

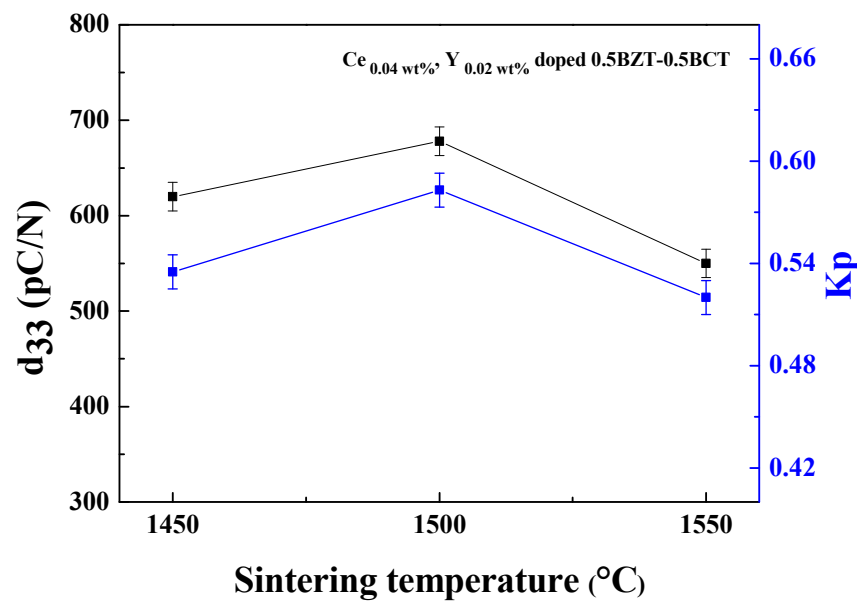


**Figure 2.** Sintering temperature dependent piezoelectric charge coefficient of  $d_{33}$  and electro-mechanical coupling coefficient of  $k_p$  of  $\text{Ce}_{0.04}\text{Y}_{0.02}\text{-(Ba}_{0.85}\text{Ca}_{0.15})(\text{Zr}_{0.1}\text{Ti}_{0.9})\text{O}_3$  ceramics.

Figure 3a,b show the X-ray diffraction patterns of  $\text{Ce}_{0.04}\text{Y}_y$  doped BCZT ceramic, and  $\text{Ce}_x\text{Y}_{0.02}$  doped BCZT ceramics, respectively. Both ceramic specimens were sintered at 1500 °C with different  $\text{CeO}_2\text{-Y}_2\text{O}_3$  contents. As shown in Figure 3, all synthesized CeY doped BCZT ceramics showed a pure perovskite structure without any pyrochlore phase. This means that  $\text{Ce}^{4+}$  and  $\text{Y}^{3+}$  cations diffused into the BCZT lattice to form a complete solid solution. As shown in Figure 3a, as the content of  $\text{Y}_2\text{O}_3$  increases, the diffraction peaks of  $\text{CeO}_2$  and  $\text{Y}_2\text{O}_3$  doped BCZT ceramics shift slightly to a higher angle. The reason for this phenomenon was the tolerance factor and radius matching rule. This can be explained from the following relational expression [18,19].

$$R_a + R_o = \sqrt{2}t (R_b + R_o) \quad (1)$$

where  $R_a$  is radius of A site,  $R_b$  is radius of B site,  $R_o$  is the oxygen ion, and  $t$  is the tolerance factor [20]. If  $t = 1$ , it means it has a cube structure. However, if  $t$  is not 1, it means that it has a certain disordered structure. As it deviates from 1, the degree of distortion increases, which has been shown to affect the stability of the  $\text{ABO}_3$  structure. Generally, it is reported that, when  $t > 0.8$ , a stable  $\text{ABO}_3$  structure can be formed [21]. The tolerance factor  $t_a$  is for the substitution of doped ions for the A site, and the tolerance factor  $t_b$  is for substitution of the doped ions for the B site, respectively. When the difference between  $t_a$  and  $t_b$  is less than 0.02, it is considered that the doped ions may enter the A site and the B site at the same time. Therefore, we may argue that small ion [ $r(\text{R}^{3+}) < 0.087$  nm] will enter the B position, and the large ion [ $r(\text{R}^{3+}) > 0.094$  nm] will enter the A position. As a result,  $\text{Y}^{3+}$  ( $r = 0.09$  nm) may enter the A site, or it may enter the B position. As shown in Figure 3c, by comparing BCZT and Ce doped BCZT ceramics, (002) and (200) peaks of Ce doped BCZT ceramics moved to the low angle. It means that lattice parameter  $c$  was increased. This increased lattice parameter indicates that the Ce ion in the BCZT- $\text{Ce}_{0.04}$  ceramic tends to occupy the B site. The reflection peaks of (002) and (200) in  $\text{Ce}_{0.04}\text{Y}_y\text{-BCZT}$  ceramic moved to a higher angle with the increase of  $y$  doping, and it can be known that  $\text{Y}^{3+}$  in the  $\text{Ce}_{0.04}\text{Y}_y\text{-BCZT}$  ceramic tends to enter the A position. As shown in Figure 3d, compared with BCZT ceramics, the reflection peak of (110) in BCZT- $\text{Y}_{0.02}$  ceramic moves to a higher angle as Y doping process. It means that lattice parameter  $a$  was decreased as increasing Y dopant. This decreased lattice parameter  $a$  indicates that the Y ion in the BCZT- $\text{Y}_{0.02}$  ceramic tends to occupy the A site, the same as when co-doping. By comparing BCZT- $\text{Y}_{0.02}$  and BCZT- $\text{Ce}_{0.02}\text{Y}_{0.02}$  ceramics, the reflection of (110) of BCZT- $\text{Ce}_{0.02}\text{Y}_{0.02}$  ceramic moves

to a higher angle and then moves to a lower angle as the content of Ce increases. It means that with the increase of Ce ions during co-doping, it first enters the A site and then enters the B site. It is somewhat different from the Ce ion occupying a place in BCZT-Ce ceramics. Since Ce ions have two valence states ( $\text{Ce}^{3+}$  (0.134 nm) and  $\text{Ce}^{4+}$  (0.087 nm)), according to the radius matching rule, large ions tend to replace large ions, and small ions tend to replace small ions. The  $\text{Ti}^{4+}$  (0.060 nm) and  $\text{Zr}^{4+}$  (0.072 nm) ions at the B site have a small radius, thus  $\text{Ce}^{4+}$  ions enter the B site, which is equivalent doping, no electronic gains, and losses, and  $\text{Ce}^{3+}$  ions enter the A site, which is the donor doping. Therefore, the co-doping of Ce and Y in  $\text{Ce}_x\text{Y}_y\text{-BCZT}$  ceramics can be regarded as double-donor doping. Moreover, in the co-doping process,  $\text{Ce}^{3+}$  ions are produced first, and then  $\text{Ce}^{4+}$  ions are produced.

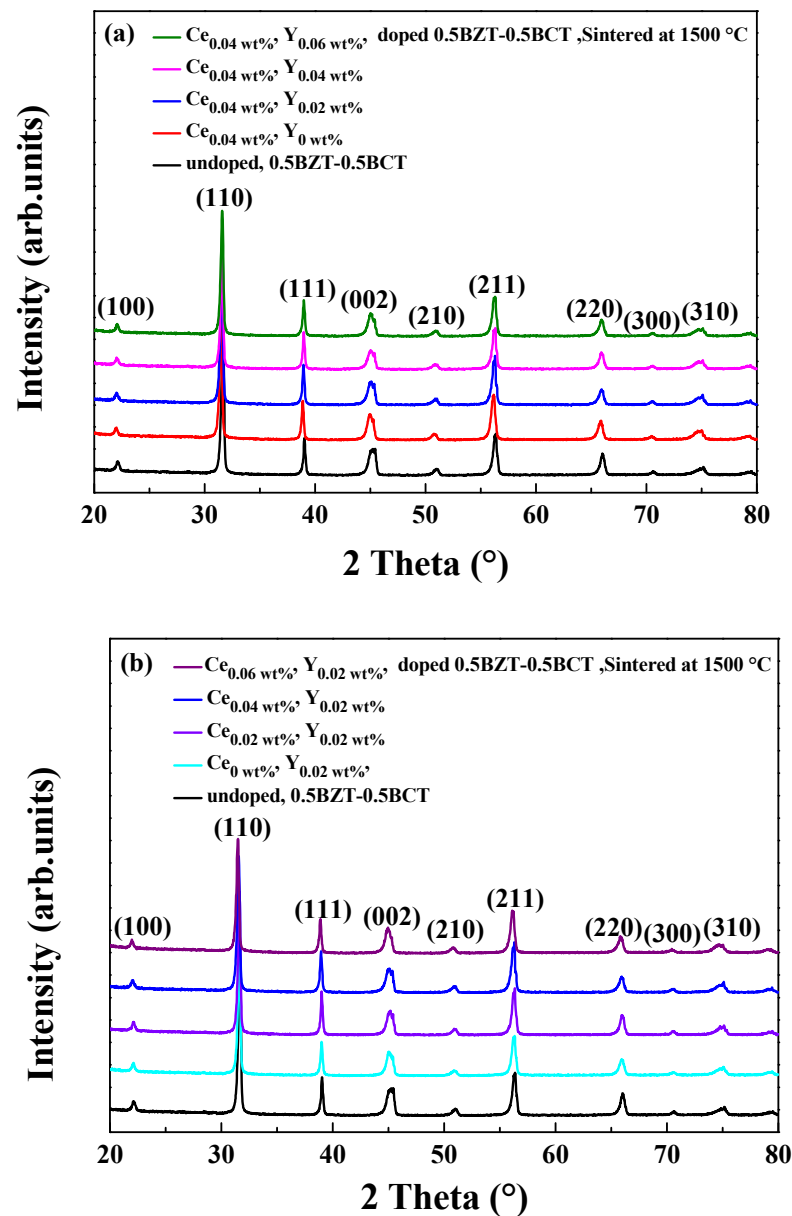
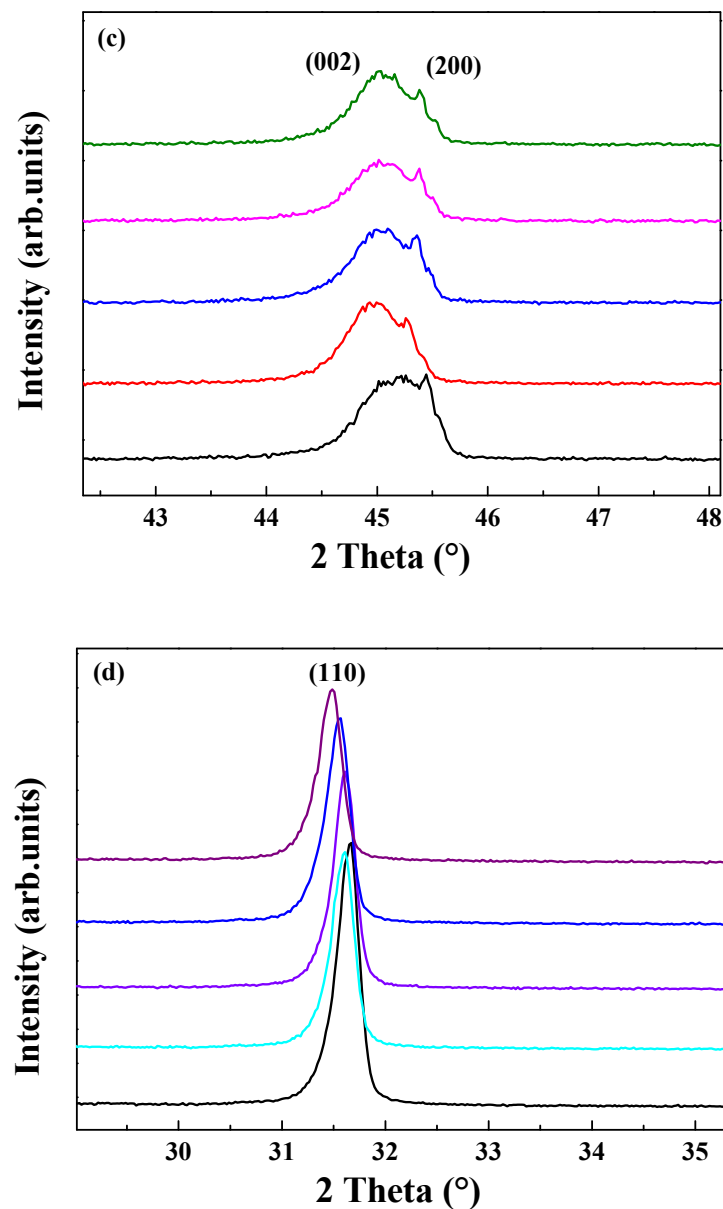
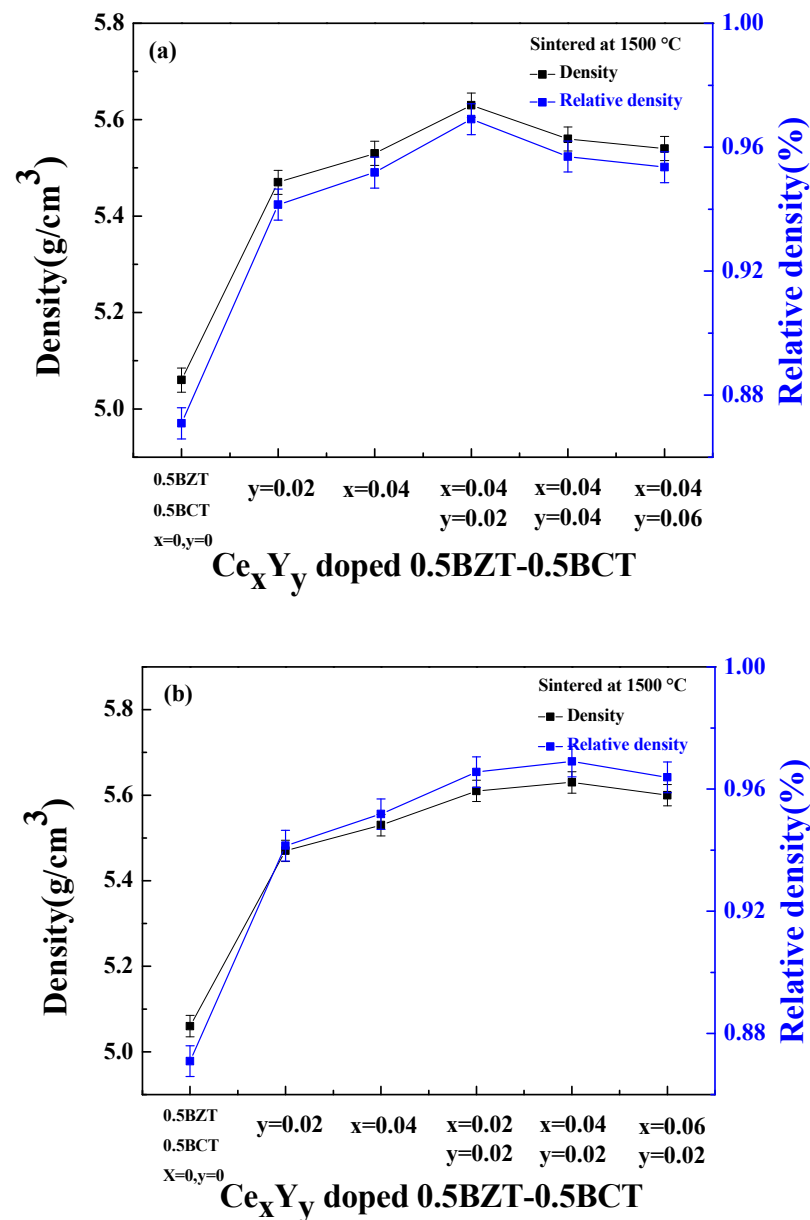


Figure 3. Cont.



**Figure 3.** (a) X-ray diffraction patterns of the  $Ce_{0.04}Y_y$  doped BCZT ceramics. (b) X-ray diffraction patterns of the  $Ce_xY_{0.02}$  doped BCZT ceramics and (c) X-ray diffraction patterns of the  $Ce_{0.04}Y_y$  doped BCZT ceramics enlarge patterns near 40–50°. (d) X-ray diffraction patterns of the  $Ce_xY_{0.02}$  doped BCZT ceramics enlarge patterns near 30–35°.

Figure 4 display the measured density of Ce and Y doped BCZT ceramics. Figure 4a shows the bulk density of  $Ce_{0.04}Y_y$  doped BCZT ceramics, which  $Y_2O_3$  contents was varied from 0.02 to 0.06, while Figure 4b displays  $Ce_xY_{0.02}$  doped BCZT ceramics, which Ce was varied from 0.02 to 0.06, respectively. It seems that the density of Ce and Y doped BCZT ceramics was related to the doped content.



**Figure 4.** The density of Ce and Y doped BCZT ceramics. (a) for the Ce<sub>0.04</sub>Y<sub>y</sub> doped BCZT ceramics, (b) Ce<sub>x</sub>Y<sub>0.02</sub> doped BCZT ceramics, respectively.

The density of ceramics is closely related to the pores and grain size [22]. It can be seen from Figure 5a,b of SEM that when the ceramic is only doped with Ce and only with Y alone, the grain size was reduced, while the density was increased due to the reduction of pores. When ceramics were co-doped, as the number of doping increases, the crystal grains gradually became larger, and the pores gradually decreased. The density of Ce<sub>0.04</sub>Y<sub>0.02</sub>-BCZT ceramics was 5.63 g/cm<sup>3</sup>, which corresponds to 96.9% of the theoretical density of BCZT ceramics of 5.81 g/cm<sup>3</sup> [23]. Figure 5c,d shows that when doped excessively, the grains grow abnormally, the holes increase, and the crystal grains decrease. The increase in relative density should be due to the increase in grain size and the decrease in porosity. However, when over-doped, the density will decrease. Although the grain size of Ce doped BCZT and Y doped BCZT ceramics have been reduced, the density has increased. This was the same as other reports that only doped Y or only Ce. We generally believe that rare-earth ions have an inhibitory effect on grain growth in perovskites because of their low diffusion rate [24]. When Ce = 0.04 wt.% Y = 0.02 wt.%, the grain size of the sample was more uniform than that of the sample without doping, the grain distribution was

more regular, and the existence of pores was also reduced. This shows that the appropriate amount of co-doping Ce-Y was helpful for grain growth. In general, the difficulty of domain movement in piezoelectric ceramics affects the piezoelectric performance. There is a great relationship between the turning of the electric domain and the growth of the crystal grains [25,26]. When excessive doping, crystal grain grows abnormally, the pores become larger, and the number of pores increases, small crystal grains are mixed between large crystal grains, and the crystal grains are squeezed and deformed, which also affects the domain wall motion [27]. The electrical properties of the sample deteriorate.

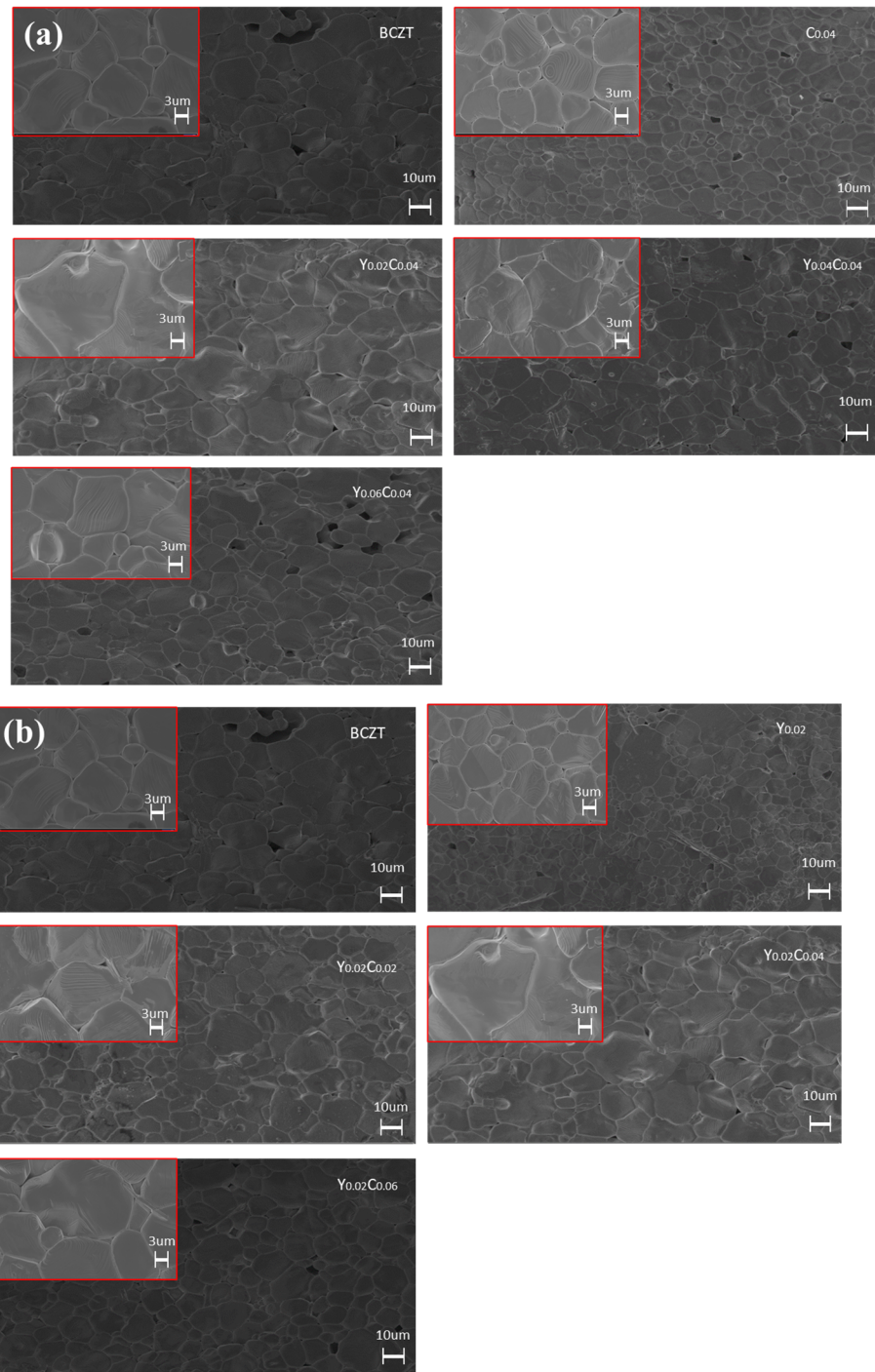
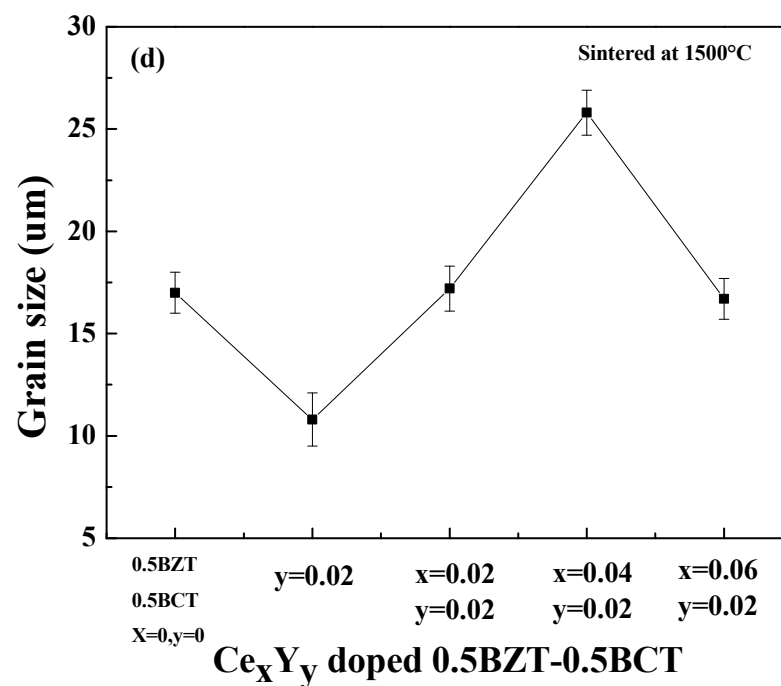
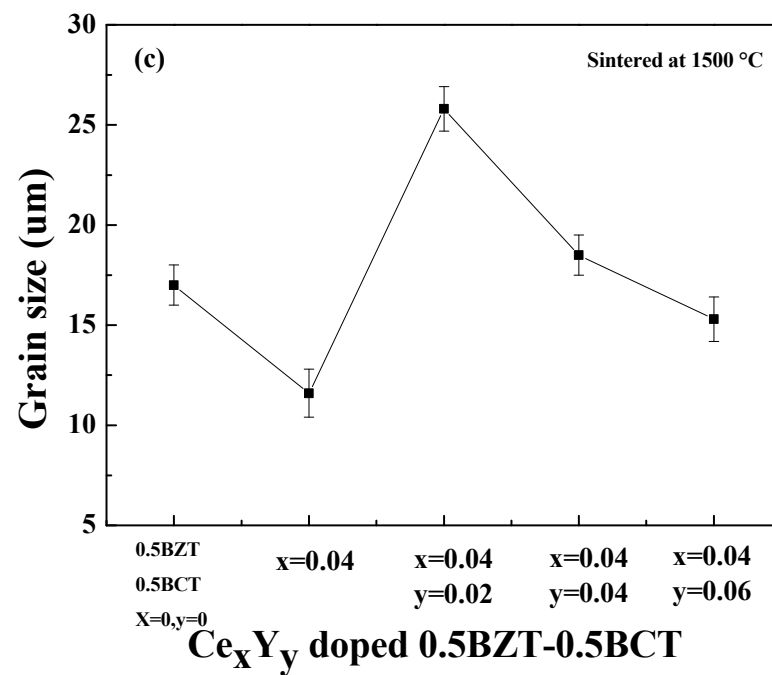


Figure 5. Cont.



**Figure 5.** The measured grain size of Ce and Y doped BCZT ceramics from the SEM images. (a) for the  $Ce_{0.04}Y_y$  doped BCZT ceramics, (b)  $Ce_xY_{0.02}$  doped BCZT ceramics, (c)  $Ce_{0.04}Y_y$  doped BCZT ceramics grain size, (d)  $Ce_xY_{0.02}$  doped BCZT ceramics grain size.

When Ce and Y dual donors were co-doped, cation vacancies were generated to maintain electrical neutrality, and cation vacancies promoted the turning of the electrical domain wall. Therefore, co-doping can increase the piezoelectric properties of ceramics, but excessive doping of Ce and Y will cause  $CeO_2$  and  $Y_2O_3$  to precipitate at the grain boundaries, refine the grains, produce pores [28], thus reducing the piezoelectric properties of the ceramic.

Figure 6 display piezoelectric charge coefficient and electro-mechanical coupling coefficient of the Ce and Y doped BCZT ceramics. (a) For the  $Ce_{0.04}Y_y$  doped BCZT

ceramics, (b)  $Ce_xY_{0.02}$  doped BCZT ceramics, respectively. As shown in Figure 6, the behavior  $d_{33}$  and  $k_p$  were very similar. As increasing the dopant, the piezoelectric charge coefficient  $d_{33}$  and electro-mechanical coupling coefficient  $k_p$  were increased. It decreased after reaching the maximum. When the Ce doping amount was 0.04 wt.% and the Y doping amount was 0.02 wt.%, the piezoelectricity of the sample the coefficient and  $k_p$  reached the highest point,  $d_{33} = 678$  pC/N,  $k_p = 0.583$ . From Figure 6, we can see that the  $k_p$  and  $d_{33}$  of co-doped ceramics were further improved compared with doping with only one element.

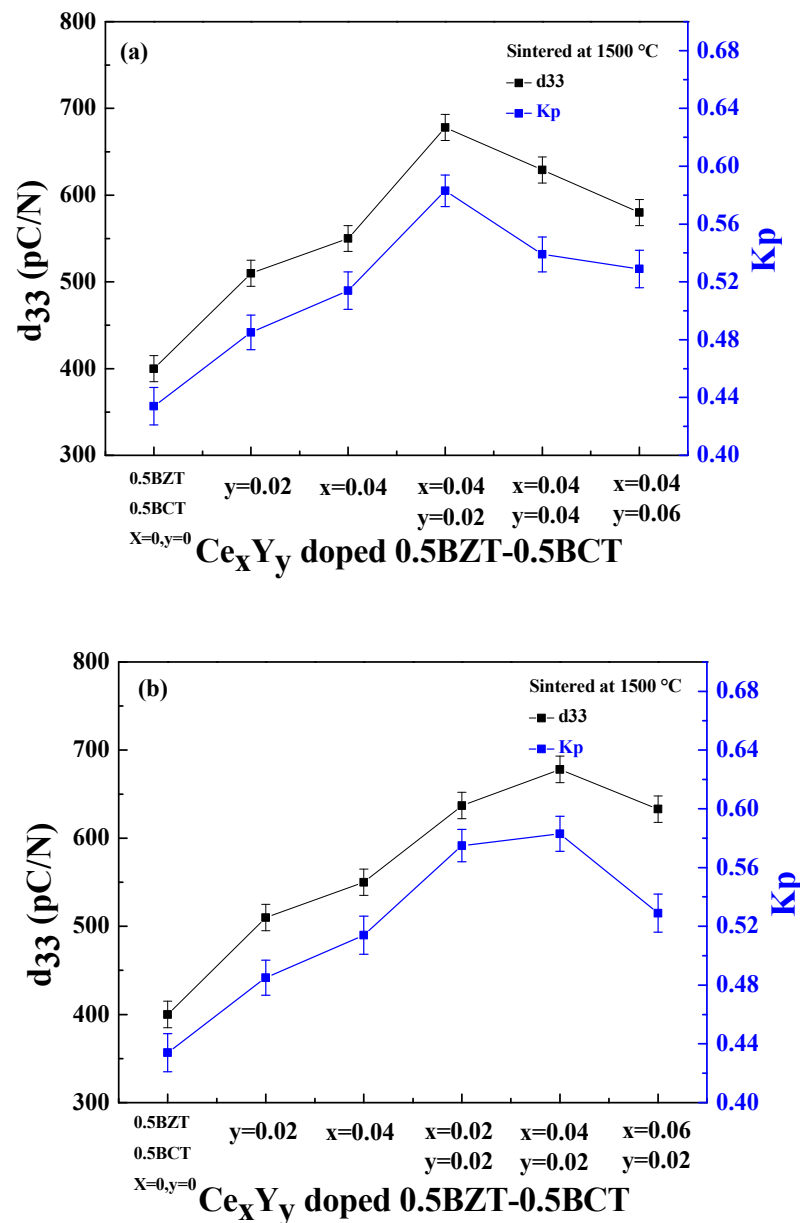


**Figure 6.** Display piezoelectric charge coefficient and electro-mechanical coupling coefficient of the Ce and Y doped BCZT ceramics. (a) For the  $Ce_{0.04}Y_y$  doped BCZT ceramics, (b)  $Ce_xY_{0.02}$  doped BCZT ceramics, respectively.

It seems that dual donor doping effects were a more effective doping method for BCZT ceramics to have higher  $k_p$  and  $d_{33}$  values. The electrical properties of piezoelectric ceramics were also closely related to the microstructure. From Figures 1 and 3, we know that the interior of the ceramic was a state where orthorhombic and tetragonal phases coexisted, and when  $Ce = 0.04$  wt.%,  $Y = 0.02$  wt.%, the ceramic density is the highest. The grain size is also large and uniform, while the number of pores is increased with small size.

This reduces the difficulty of domain turning. Therefore,  $Ce_{0.04}Y_{0.02}$  doped BCZT ceramics showed the highest piezoelectric performance in this research.

Figure 7a,b shows the schematic diagrams of the piezoelectric energy harvesting system and their equivalent circuit for the piezoelectric ceramics, respectively. By operating the energy harvesting system by the controlling system, a pressure of 200 N was applied through the mechanical force system with 0.25 Hz. Oscilloscope was employed to record generated output voltages in BCZT-CY ceramic.

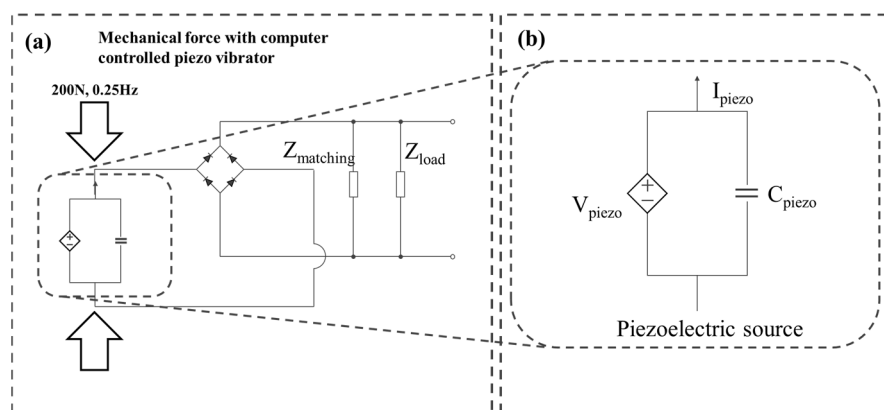


**Figure 7.** (a) The schematic diagram of the piezoelectric energy harvesting system. (b) Detailed equivalent images of piezoelectric source part in (a).

As shown in Figure 8, voltages meant that generated output voltages in the piezoelectric energy harvesters were made of (a)  $Ce_{0.04}Y_y$  doped BCZT ceramic and (b)  $Ce_xY_{0.02}$  doped BCZT ceramics, respectively. The generated piezoelectric output voltage was important for energy harvesting, which represents the electrical energy generated by the ceramic when pressure was applied, which can be explained by the following formula.

$$g_{33} = d_{33} / \epsilon_r \epsilon_0 \tag{2}$$

$$V = (g_{33}hT) \tag{3}$$

The  $g_{33}$  is the piezoelectric voltage constant,  $\epsilon_0$  is the dielectric constant measured under vacuum conditions,  $\epsilon_r$  is the dielectric constant of the ceramic in the air [29].  $V$  is the voltage generated when pressure is applied to the ceramic,  $h$  is the ceramic thickness, and  $T$  is the stress [30]. As shown in Equations (2) and (3), generated output voltage can be controlled by the piezoelectric properties of  $g_{33}$ , devices structural parameter of  $h$ , and applied stress of  $T$ , respectively. Figure 8 displays the open-circuit voltage generated by applying a force of 200 N in a 0.25 Hz environment, the open-circuit voltage measured by BCZT- $Ce_{0.04}Y_{0.02}$  ceramics was 8.9 V, the highest value among BCZT- $Ce_xY_y$  ceramics. Figure 8 displays the behavior of the open-circuit voltage was very consistent with  $d_{33}$  in Figure 6, and it can be seen from formula (2) that the greater the value of  $d_{33}$ , the greater the voltage generated when pressure was applied.

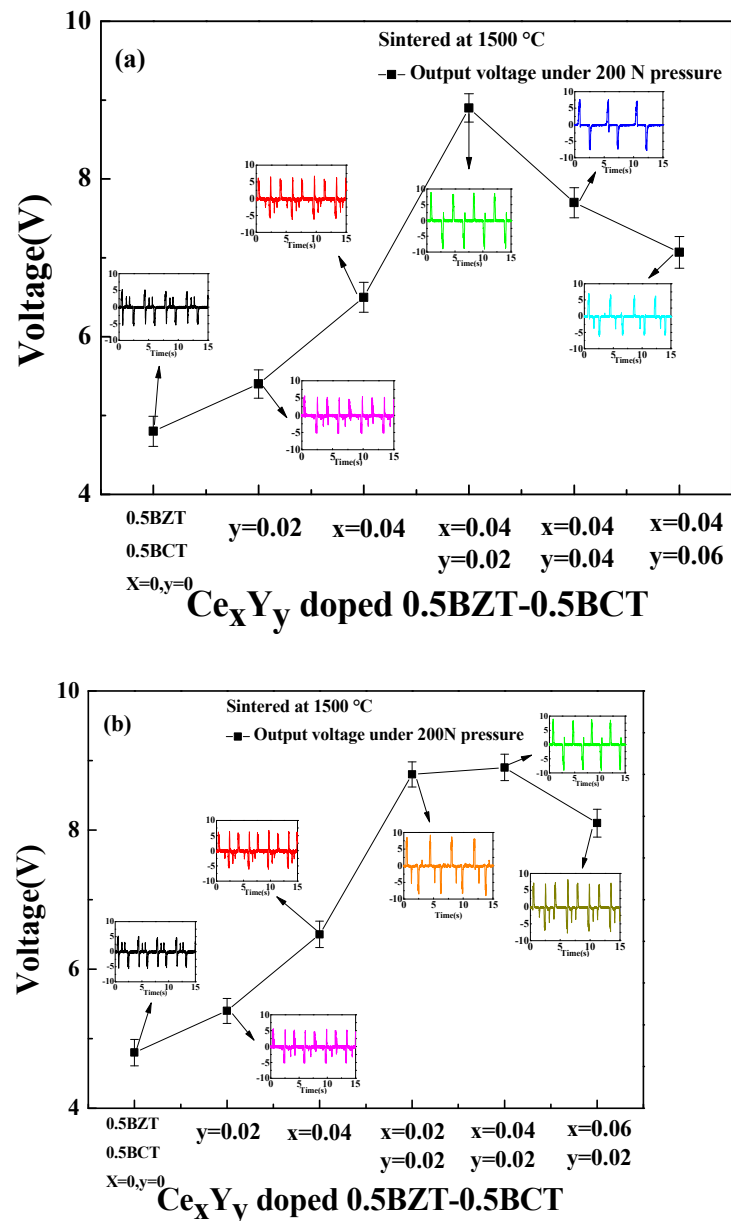


**Figure 8.** Generated output voltage in the BCZT-CY ceramics ceramic after applying a pressure of 200 N. (a) For the  $Ce_{0.04}Y_y$  doped BCZT ceramics, (b)  $Ce_xY_{0.02}$  doped BCZT ceramics, respectively.

#### 4. Conclusions

In this study,  $(Ba_{0.85}Ca_{0.15})(Zr_{0.1}Ti_{0.9})O_3$  ceramics with dual donor doping effects were prepared by co-doping Ce and Y. A small amount of CeY co-doping can significantly improve the performance of  $(Ba_{0.85}Ca_{0.15})(Zr_{0.1}Ti_{0.9})O_3$  ceramics. The effects of different contents of  $CeO_2$ - $Y_2O_3$  dopants to the  $(Ba_{0.85}Ca_{0.15})(Zr_{0.1}Ti_{0.9})O_3$  composition were analyzed by studying the phase, surface microstructure, piezoelectric, and ferroelectric properties of BCZT ceramics. By optimizing the co-doping process of  $CeO_2$  and  $Y_2O_3$  to  $(Ba_{0.85}Ca_{0.15})(Zr_{0.1}Ti_{0.9})O_3$  ceramics, piezoelectric and electro-mechanical properties were improved. Moreover, these dopants can promote the grain growth process in  $(Ba_{0.85}Ca_{0.15})(Zr_{0.1}Ti_{0.9})O_3$  ceramics.  $Ce_{0.04}Y_{0.02}$  doped  $(Ba_{0.85}Ca_{0.15})(Zr_{0.1}Ti_{0.9})O_3$  ceramic showed the highest piezoelectric properties compared with other composition, the results were as follows: relative density = 96.9%,  $K_p = 0.583$ , and  $d_{33} = 678$  pC/N,  $V = 8.9$  V. It means that this  $Ce_{0.04}Y_{0.02}$  doped  $(Ba_{0.85}Ca_{0.15})(Zr_{0.1}Ti_{0.9})O_3$  ceramic was a desired material in the application of lead-free ceramics. Since  $(Ba_{0.85}Ca_{0.15})(Zr_{0.1}Ti_{0.9})O_3$  piezoelectric materials have excellent piezoelectric properties such as piezoelectric charge coefficient  $d_{33}$

of 678 pC/N with high density, divided ingredients of piezoelectric components can be applied for the flexible device applications. By connecting by the gride line, this divided ingredient of piezoelectric components can be applied for flexible device applications.

**Author Contributions:** Data curation, C.L.; formal analysis, C.L. and J.-H.K.; investigation, C.L.; project administration, J.-H.K.; validation, C.L.; writing—original draft C.L. and J.-S.B.; writing—review and editing, C.L. and J.-H.K. All authors have read and agreed to the published version of the manuscript.

**Funding:** This research was supported by the MSIT (Ministry of Science and ICT), Korea, under the ITRC (Information Technology Research Center) support program (IITP-2021-2020-0-01655) supervised by the IITP (Institute of Information and Communications Technology Planning and Evaluation) and supported by the Chung-Ang University Young Scientist Scholarship in 2020 (admission year).

**Institutional Review Board Statement:** Not applicable.

**Informed Consent Statement:** Not applicable.

**Data Availability Statement:** The data presented in this study are available on request from the corresponding author.

**Conflicts of Interest:** The authors declare no conflict of interest.

## References

- Haertling, H.K. Ferroelectric ceramics: History and technology. *J. Am. Ceram. Soc.* **1999**, *82*, 797–818. [[CrossRef](#)]
- Panda, K.P. Review: Environmental friendly lead-free piezoelectric materials. *J. Mater. Sci.* **2009**, *44*, 5049–5062. [[CrossRef](#)]
- Rödel, J.; Jo, W.; Seifert, K.T.P.; Anton, E.M.; Granzow, T. Perspective on the development of lead-free piezoceramics. *J. Am. Ceram. Soc.* **2009**, *92*, 1153–1177. [[CrossRef](#)]
- Shrout, T.R.; Zhang, S.J. Lead-free piezoelectric ceramics: Alternatives for PZT? *J. Electroceram.* **2007**, *19*, 111–124. [[CrossRef](#)]
- Clementi, G.; Margueron, S.; Suarez, M.A.; Baron, T.; Dulmet, B.; Bartaszyte, A. Piezoelectric and pyroelectric energy harvesting from lithium niobate films. *J. Phys. Conf. Ser.* **2019**, *1407*, 012039. [[CrossRef](#)]
- Kalimuldina, G.; Turdakyn, N.; Abay, I.; Medeubayev, A.; Nurpeissova, A.; Adair, D.; Bakenov, Z. A Review of Piezoelectric PVDF Film by electrospinning and its applications. *Sensors* **2020**, *20*, 5214. [[CrossRef](#)] [[PubMed](#)]
- Acosta, M.; Novak, N.; Rojas, V.; Patel, S.; Vaish, R.; Koruza, J.; Rossetti, G.A., Jr.; Rodel, J. BaTiO<sub>3</sub>-based piezoelectrics: Fundamentals, current status, and perspectives. *Appl. Phys. Rev.* **2017**, *4*, 041305. [[CrossRef](#)]
- Mariello, M.; Fachechi, L.; Guido, F.; Vittorio, M.D. Multifunctional sub-100 μm thickness flexible piezo/triboelectric hybrid water energy harvester based on biocompatible AlN and soft parylene C-PDMS-Ecoflex™. *Nano Energy* **2021**, *83*, 2211–2855. [[CrossRef](#)]
- Mariello, M.; Qualtieri, A.; Mele, G.; Vittorio, M.D. Metal-free multilayer hybrid peng based on soft electrospun/sprayed membranes with cardanol additive for harvesting energy from surgical face masks. *ACS Appl. Mater. Interfaces* **2021**, *13*, 20606–20621. [[CrossRef](#)]
- Cui, Y.R.; Yuan, C.L.; Liu, X.Y.; Zhao, X.Y.; Shan, X. Lead-free (Ba<sub>0.85</sub>Ca<sub>0.15</sub>)(Ti<sub>0.9</sub>Zr<sub>0.1</sub>)O<sub>3</sub>-Y<sub>2</sub>O<sub>3</sub> ceramics with large piezoelectric coefficient obtained by low-temperature sintering. *J. Mater. Sci. Mater. Electron.* **2013**, *24*, 654–657. [[CrossRef](#)]
- Li, W.; Xu, Z.; Chu, R.; Fu, P.; Peng, A. Effect of Ho doping on piezoelectric properties of BCZT ceramics. *Ceram. Int.* **2012**, *38*, 4353–4355. [[CrossRef](#)]
- Liu, W.; Ren, X. Large Piezoelectric Effect in Pb-Free Ceramics. *PRL* **2009**, *103*, 257602. [[CrossRef](#)] [[PubMed](#)]
- Ji, X.; Wang, C.B.; Harumoto, T.; Zhang, S.; Tu, R.; She, Q.; Shi, J. Structure and electrical properties of BCZT ceramics derived from microwave-assisted sol-gel-hydrothermal synthesized powders. *Sci. Rep.* **2020**, *10*, 20352. [[CrossRef](#)] [[PubMed](#)]
- Parjansri, P.; Intatha, U.; Eitsayeam, S. Dielectric, ferroelectric and piezoelectric properties of Nb<sup>5+</sup> doped BCZT ceramics. *Mater. Res. Bull.* **2015**, *65*, 61–67. [[CrossRef](#)]
- Wang, L.; Bai, W.; Zhao, X.; Ding, Y.; Wu, S.; Zheng, P.; Li, P.; Zhai, J. Influences of rare earth site engineering on piezo electric and electromechanical response of (Ba<sub>0.85</sub>Ca<sub>0.15</sub>)(Zr<sub>0.1</sub>Ti<sub>0.9</sub>)O<sub>3</sub> lead-free ceramics. *Mater. Electron.* **2020**, *31*, 6560–6573. [[CrossRef](#)]
- Liu, X.; Chen, Z.; Fang, B.; Ding, J.; Zhao, X.; Xu, H.; Luo, H. Enhancing piezoelectric properties of BCZT ceramics by Sr and Sn co-doping. *J. Alloy. Compd.* **2015**, *640*, 128–133. [[CrossRef](#)]
- Rahaman, M.N. *Ceramic Processing and Sintering*, 2nd ed.; CRC Press: Boca Raton, FL, USA, 2003.
- Bijalwan, V.; Hughes, H.; Pooladvand, H.; Tofel, P.; Nan, B.; Holcmanc, V.; Bai, Y.; Buttona, T.W. The effect of sintering temperature on the microstructure and functional properties of BCZT-xCeO<sub>2</sub> lead free ceramics. *Mater. Res. Bull.* **2019**, *114*, 121–129. [[CrossRef](#)]
- Gao, D.; Kwok, K.W.; Lin, D.; Chan, H.L.W. Microstructure, electrical properties of CeO<sub>2</sub>-doped (K<sub>0.5</sub>Na<sub>0.5</sub>)NbO<sub>3</sub> lead-free piezoelectric ceramic. *J. Mater. Sci.* **2009**, *44*, 2466–2470. [[CrossRef](#)]
- Tsur, Y.; Ddunbar, T.D.; Randall, C.A. Crystal and defect chemistry of rare earth cations in BaTiO<sub>3</sub>. *J. Electroceram.* **2001**, *7*, 25–34. [[CrossRef](#)]

21. Liu, X.C.; Hong, R.Z.; Tian, C.S. Tolerance factor and the stability discussion of  $ABO_3$ -type ilmenite. *J. Mater. Sci.* **2009**, *20*, 323–327. [[CrossRef](#)]
22. Kang, S.J.L. *Elsevier Sintering, Densification, Grain Growth and Microstructure*; Butterworth-Heinemann Publication: Oxford, UK, 2005; pp. 89–135.
23. Buatip, N.; Promsawat, N.; Pisitpipathsin, N.; Namsar, O.; Pawasri, P.; Ounsung, P.; Phabsimma, K.; Rattanachan, S.T.; Janphuang, P.; Projprapai, S. Investigation on electrical properties of BCZT ferroelectric ceramics prepared at various sintering condition. *Integr. Ferroelectr.* **2018**, *187*, 45–52. [[CrossRef](#)]
24. Cui, Y.; Liu, X.; Jiang, M.; Zhao, X.; Shan, X.; Li, W.; Yuan, C.; Zhou, C. Lead-free  $(Ba_{0.85}Ca_{0.15})(Ti_{0.9}Zr_{0.1})O_3$ - $CeO_2$  ceramics with high piezoelectric coefficient obtained by low-temperature sintering. *Ceram. Int.* **2012**, *38*, 4761–4764. [[CrossRef](#)]
25. Gunnar, P.; Khansur, N.H.; Webber, K.G.; Kungl, H.; Hoffmann, M.J.; Hinterstein, M. Grain size effects in donor doped lead zirconate titanate ceramics. *J. Appl. Phys.* **2020**, *128*, 214105.
26. Ștefan, Ț. *Micro and Nanoscale Characterization of Three Dimensional Surfaces. Basics and Applications*; Napoca Star Publishing House: Cluj-Napoca, Romania, 2015; pp. 21–27.
27. Ghosh, D.; Sakata, A.; Carter, J.; Thomas, P.A.; Han, H.; Nino, J.C.; Jones, J.L. Domain wall displacement is the origin of superior permittivity and piezoelectricity in  $BaTiO_3$  at intermediate grain sizes. *Adv. Funct. Mater.* **2014**, *24*, 885–896. [[CrossRef](#)]
28. Du, G.; Wei, F.; Li, W.; Chen, N. Co-doping effects of A-site  $Y^{3+}$  and B-site  $Al^{3+}$  on the microstructures and dielectric properties of  $CaCu_3Ti_4O_{12}$  ceramics. *J. Eur. Ceram. Soc.* **2017**, *37*, 4653–4659. [[CrossRef](#)]
29. Yan, X.-D.; Zheng, M.-P.; Zhu, M.; Hou, Y.-D. Soft and hard piezoelectric ceramics for vibration energy harvesting. *Crystals* **2020**, *10*, 907. [[CrossRef](#)]
30. Shin, D.J.; Kim, J.-W.; Koh, J.H. Piezoelectric properties of  $(1-x)BZT-xBCT$  system for energy harvesting applications. *J. Eur. Ceram. Soc.* **2018**, *38*, 4395–4403. [[CrossRef](#)]